Macromolecules **2003,** *36,* 7301−7307

Photoluminescence and Electroluminescence Study of Violet-Blue and Green Emitting Polymers and Their Blend

Liming Ding,[†] Frank E. Karasz,* Yao Lin,[†] Yi Pang,[‡] and Liang Liao[‡]

Department of Polymer Science & Engineering, University of Massachusetts,
Amherst, Massachusetts 01003, and Department of Chemistry, Clark Atlanta University,
Atlanta, Georgia 30314

Received April 21, 2003; Revised Manuscript Received July 21, 2003

ABSTRACT: The photoluminescence and electroluminescence of violet-blue (**I**) and green (**II**) emitting polymers and their blend were studied. This included the effects of excitation wavelength, concentration, and film thickness on the photoluminescence; also, double-layer LEDs (ITO/PEDOT/polymer/Ca/Al) were fabricated and compared with single-layer LEDs. For the first time a strong dependence of the PL spectra on excitation wavelength for a violet-blue polymer in solution was observed. When the applied voltage was increased, the EL spectra showed a blue shift, and the emission intensity for the observed higher energy transition increased at the expense of the lower energy transition. Förster energy transfer in the photoluminescence and electroluminescence of the polymer blend was also studied. The results indicate that the energy transfer was independent of excitation wavelength and applied voltage. The LED using the blend was found to be more efficient than either of the devices using polymers **I** or **II**, because polymer **I** provides excitons which migrate to the chain of polymer **II** and contribute to the total emission. Furthermore, polymer **I** acts as a diluent to reduce exciton quenching. The chromophore blend also aids the separation of PL output from absorption, thereby alleviating self-absorption and improving the device efficiency.

Introduction

Light-emitting diodes based on conjugated polymers[1] have been studied for more than 1 decade.[2] Research has been carried out with the objective of chemically tuning the emission color of conjugated polymers[3−5] and improving the quantum efficiency, stability, and lifetimes.[6−8] Currently, conjugated polymers also find other applications in light-emitting electrochemical cells (LECs),[9] photodiodes,[10] transistors,[11] and lasers.[12] The class of materials has the advantage of a facile color tunability, of good film-forming property, and of adequate mechanical properties in comparison to inorganic semiconductors.

Tuning the chemical structure and band gap of conjugated polymers and designing LEDs emitting selected colors remains a challenging issue. Up to now five strategies have been reported for tuning the emission color of polymer LEDs: changing the main-chain molecular structure,[13,14] changing the side-chain molecular structure,[15] blending a light-emitting polymer with another polymer[16,17] or with small organic[18] or inorganic molecules,[19] doping,[20] and using multilayer architectures.[21] Polymer blending provides a simple, low-cost, and often very effective way to obtain new chromophores for use in LEDs. By carefully selecting different luminescent polymers for blending and by controlling the content of the target chromophore in the blend, one may obtain different emission colors with reasonable quantum efficiency.[22,23] In all the PL and EL studies of conjugated polymer blends, singlet exciton transfer (Förster energy transfer)[24] has been of great interest. By controlling or using Förster energy transfer,[25,26] one can control the emission color of LEDs, obtain white LEDs,[27−30] or reduce the optical losses in polymer laser engineering.[31] Many other investigations focusing on energy transfer have been reported, including energy transfer between polymers and organic metal complexes,[32,33] between oligomers,[34] controlling energy transfer by embedding MEH−PPV chains in the channels of an ordered mesoporous silica glass,[35] and depolarizing energy transfer.[36]

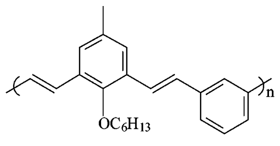

Polymer **I**

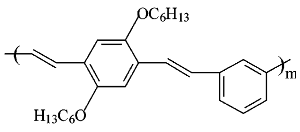

Polymer **II**

Figure 1. Structures for polymers **I** and **II**.

In this paper, we present studies of photoluminescence (PL) and electroluminescence (EL) for two conjugated polymers (Figure 1) and their blend. The effect of excitation wavelength, concentration and film thickness on the PL was investigated. Förster energy transfer in PL and EL of the polymer blend is discussed.

Experimental Section

The violet-blue emitting polymer (**I**) and green emitting polymer (**II**) were synthesized according to the procedures described previously.[37,38] PL spectra were recorded on a Perkin-

---

* Corresponding author: e-mail fekarasz@polysci.umass.edu.
[†] University of Massachusetts.
[‡] Clark Atlanta University.

10.1021/ma030237q CCC: $25.00

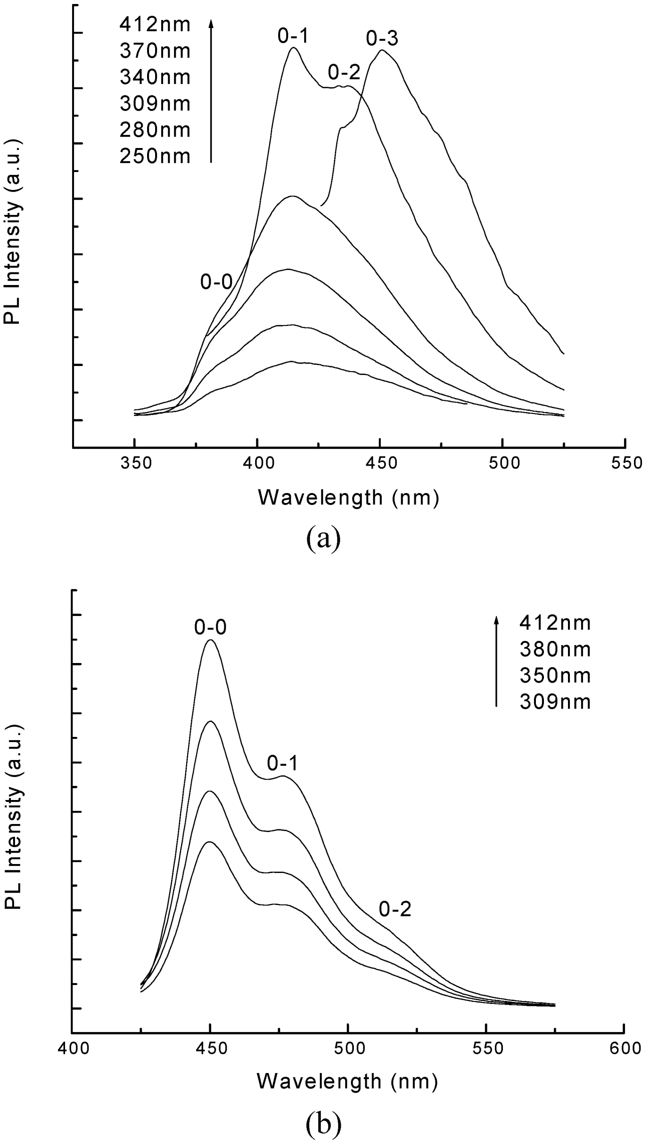

(a)

(b)

Figure 2. PL spectra of 1 × 10^{-4} mg/mL polymer/chloroform solution under different excitation wavelengths: (a) polymer **I** solution; (b) polymer **II** solution. Inserts show the excitation wavelength.

Elmer LS 50B luminescence spectrometer using a xenon discharge lamp for excitation. PEDOT/PSS (Bayer Co.) was spin-cast onto ITO glass (OFC Co.) used as the anode. The polymer solutions (20 mg/mL in chloroform) were filtered through 0.2 μm Millex-FGS Filters (Millipore Co.), and were spin-cast onto dried PEDOT/ITO substrates under a nitrogen atmosphere. The polymer films were typically 75 nm thick. Calcium electrodes of 400 nm thickness were evaporated onto the polymer films at about 10^{-7} Torr, followed by a protective coating of aluminum. The devices were characterized using a system constructed in our laboratory described elsewhere.[21] AFM was performed with a NanoScope IIIa (Digital Instruments) in the tapping mode. UV−vis spectra were recorded on a HITACHI U-3010 UV/vis spectrophotometer.

Results and Discussion

Effect of Excitation Wavelength on Photoluminescence. The photoluminescence spectra for 1 × 10^{-4} mg/mL chloroform solution of polymers **I** and **II** under different excitation wavelengths are shown in Figure 2, parts a and b, respectively. The peak wavelengths are listed in Tables 1 and 2. With an increase of excitation wavelength the PL spectra show a red shift which can be attributed to a strong correspondence between excitation energy and the vibronic structure of the emission spectra. In the emission spectra using excitation at 220 and 250 nm, the peaks at 384 and 385 nm reflect the 0−0 transition; the 412 and 414 nm peaks, the 0−1 transition. The absorption maximum wavelength for polymer **I**/chloroform solution is 309 nm. When 280, 309, and 340 nm were used as the excitation wavelengths, the emission from the 0−1 transition was dominant and the spectra overlap the contribution from the 0−0 transition. When 370 nm was used as the excitation wavelength, the emission spectrum was resolved into two peaks, 415 and 435 nm, which can be attributed to the 0−1 and 0−2 transitions, respectively. When the solution was excited with 412 nm light, the emission spectrum shows a quite different shape with 451 nm as the main peak and a shoulder at 435 nm. The former can be attributed to the 0−3 transition. This indicates that under higher excitation wavelength the lower energy transition will dominate the emission at the expense of the emissions from the higher energy transitions. The red shift in the PL at longer excitation wavelength is also affected by the band gap distribution in the polymer; at longer excitation wavelengths, the lower band gap segments will contribute more to the emission.

Table 1. Photoluminescence of 1 × 10^{-4} mg/mL Polymer I/Chloroform Solution under Different Excitation Wavelength

excitation wavelength (nm)	λ_{max}^{PL}(nm)			
	0−0	0−1	0−2	0−3[a]
220	384	**412**[c]		
250	385	**414**		
280		**414**		
309[b]		**412**		
340		**414**		
370		**415**	435	
412[b]			435	**451**
500		no emission		

[a] Vibronic transitions. [b] 309 and 412 nm are the absorption peak wavelengths of polymers **I** and **II** respectively. [c] Bold data indicate the main peak.

Table 2. Photoluminescence of 1 × 10^{-4} mg/mL Polymer II/Chloroform Solution under Different Excitation Wavelengths

excitation wavelength (nm)	λ_{max}^{PL}(nm)		
	0−0	0−1	0−2
309	**450**	473	517
350	**450**	473	517
380	**450**	475	518
412	**450**	477	518
500		emission very weak	

[c] Bold data indicate the main peak.

With an increase of excitation wavelength, the emission spectra of polymer **II** solution similarly show a small red shift. The 450, 473−477, and 517−518 nm peaks can be attributed to the 0−0, 0−1, and 0−2 vibronic transitions, respectively. Compared with polymer **I**, the emission spectra of polymer **II** are less sensitive to the excitation wavelength. From 309 to 412 nm, the emission intensity ratio between the 0−0 and the 0−1 transitions is constant at 1.6. This indicates that the vibronic structures of the emission spectra for the lower band-gap polymer (**II**) are more stable than

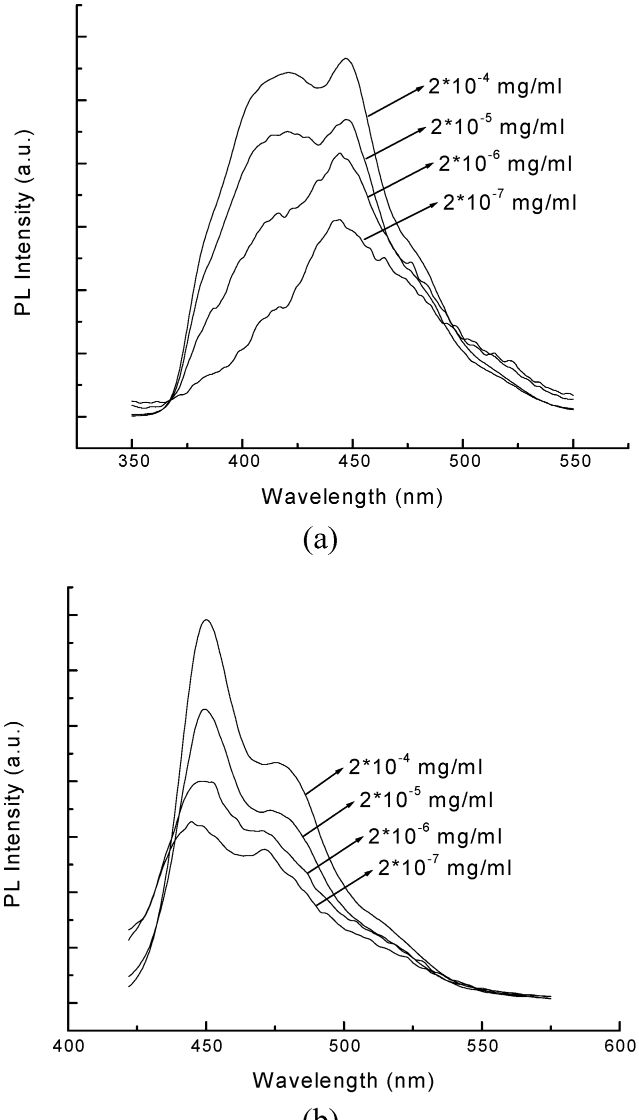

Figure 3. PL spectra for polymer blend(1:1)/chloroform solution with different concentration. Excitation wavelength: (a) 309 nm; (b) 412 nm.

that for the high band-gap polymer (**I**) under photoexcitation.

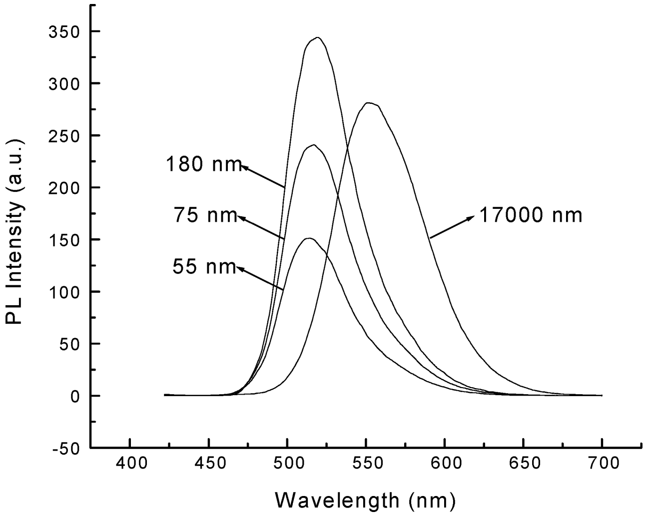

Figure 4. PL spectra of polymer **II** films spin-coated from 20 mg/mL chloroform solution. The PL spectrum of a directly cast film is shown for comparison. Excitation wavelength 412 nm.

Table 3. Photoluminescence of Polymer Blend (1:1)/ Chloroform Solution with Different Concentration under Different Excitation Wavelength

concentration (mg/mL)	$\lambda_{\max}^{\mathrm{PL}}$ (nm)
(a) 309 nm Excitation	
2×10^{-7}	417, **444**
2×10^{-6}	417, **444**
2×10^{-5}	421, **447**
2×10^{-4}	421, **447**
(b) 412 nm Excitation	
2×10^{-7}	**445**, 468
2×10^{-6}	**449**, 470
2×10^{-5}	**450**, 473
2×10^{-4}	**450**, 475

[c] Bold data indicate the main peak.

Table 4. Photoluminescence of Polymer II Films with Different Thicknesses under 412 nm Excitation Wavelength

thickness (nm)	$\lambda_{\max}^{\mathrm{PL}}$ (nm)
55[a]	514
75[a]	517
180[a]	519
17 000[b]	551

[a] Spin-coating films. [b] Cast film.

Table 5. Photoluminescence of a Polymer Blend (1:1) Film. Comparison with Polymer I and II Films

polymer	$\lambda_{\max}^{\mathrm{PL}}$ (nm)[c]
I[a]	**439**, 459
II[b]	**514**
blend[a]	**507**
blend[b]	**507**

[a] 306 nm excitation wavelength. [b] 412 nm excitation wavelength. [c] Bold data indicate the main peak.

Effect of Concentration on Photoluminescence. Photoluminescence spectra for a polymer blend (**I**:**II** = 1:1, weight ratio) in chloroform solution with different concentrations are shown in Figure 3; the PL peak wavelengths are listed in Table 3. With the increase of polymer concentration, the PL spectra show a red shift. This is due to intermolecular excimer formation.[39,40] As indicated by Chandross et al.,[41,42] the excimer, a sandwich dimer, is formed by the interaction of a ground-state molecule with an excited molecule. The absorption peak wavelengths for polymers **I** and **II** (309 and 412 nm, respectively) were used as the excitation wavelengths. In Figure 3a, peaks at 417−421 nm reflecting the 0−1 transition of polymer **I**, and at 444−447 nm the 0−0 transition of polymer **II** are seen. In Figure 3b, 445−450 nm and 468−475 nm peaks are associated with the 0−0 and 0−1 transition of polymer **II**. Figure 3 indicates that the PL spectra of the polymer blend solution were highly dependent on the excitation wavelength. At 309 nm excitation, the PL spectra of the polymer blend solutions show a combination of emissions from the two polymers. However, when 412 nm excitation was used, the polymer blend solution only shows emission from polymer **II**, because the 451 nm emission (i.e., the 0−3 transition) from polymer **I** is too weak and is overlapped by the stronger emission from polymer **II**. These results indicate that Förster energy transfer from the high band gap polymer **I** to the lower band gap polymer **II** does not occur in very dilute solution, since **I** and **II** molecules are too distant from each other.

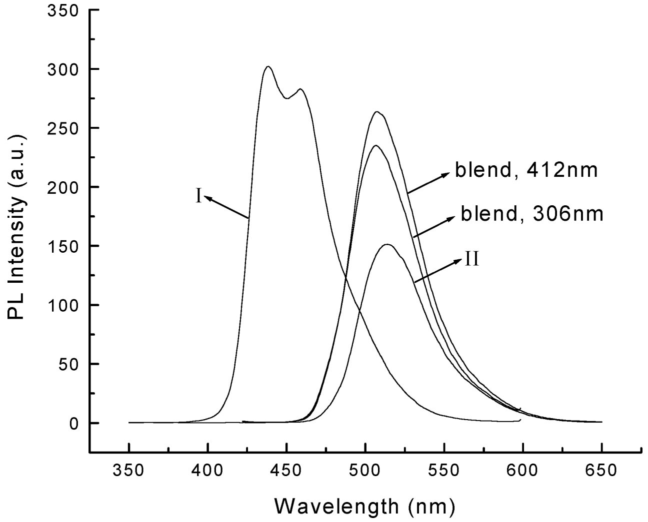

Figure 5. PL spectra of solid films of polymer **I**, **II** and blend (1:1). The blend film was excited with different wavelengths (306 or 412 nm) for comparison.

Table 6. Electroluminescence of LEDs Using Polymer Blend (1:1). Comparison with LEDs Using Polymers I and II[a]

	$\lambda_{\max}{}^{EL}$ (nm)	
polymer	single-layer	double-layer
I	438, **454**	448, **464**
II	**512**, 529	514, **522**
blend	**510**, 529	**513**, 531

[a] Bold data indicate the main peak.

Table 7. EL Peak Wavelengths at Different Voltages[a]

voltage (V)	$\lambda_{\max}{}^{EL}$ (nm)
(a) ITO/PEDOT/**I**/Ca	
8	448, **464**
10	**444**, 461
(b) ITO/**II**/Ca	
8	518, **537**
9	**516**, 530
10	**512**, 529
(c) ITO/PEDOT/**II**/Ca	
5	517, **531**
7	514, **522**
(d) ITO/PEDOT/blend/Ca	
5	**517**, 531
6	**514**, 531
7	**513**, 530
8	**506**, 521

[a] Bold data indicate the main peak.

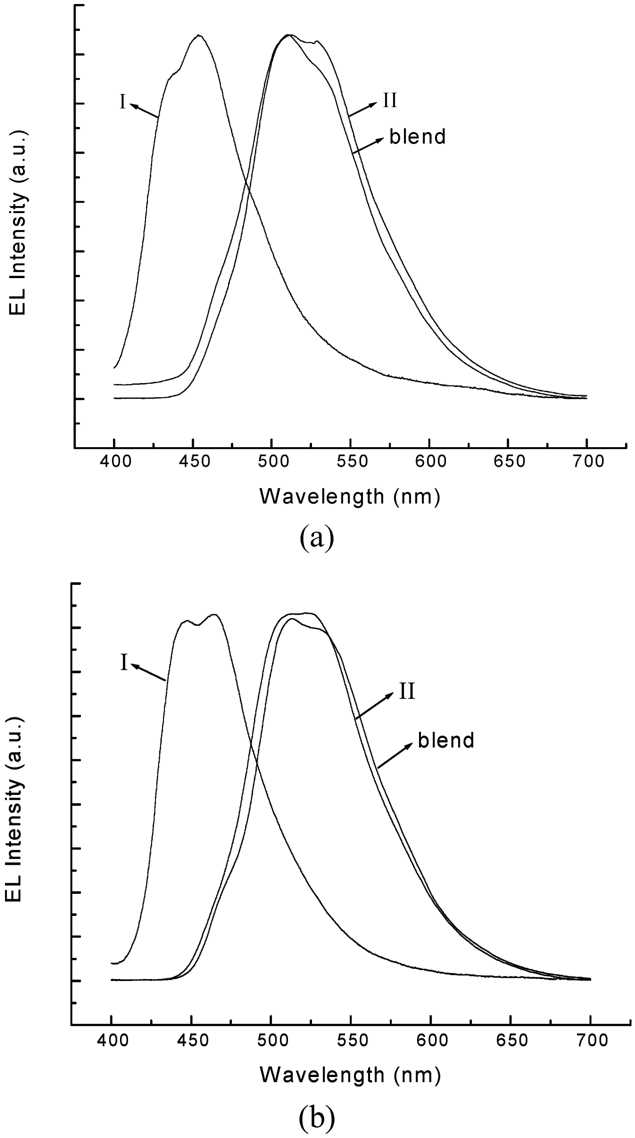

(a)

(b)

Figure 6. Electroluminescence spectra: (a) single-layer ITO/Polymer/Ca devices; (b) double-layer ITO/PEDOT/Polymer/Ca devices.

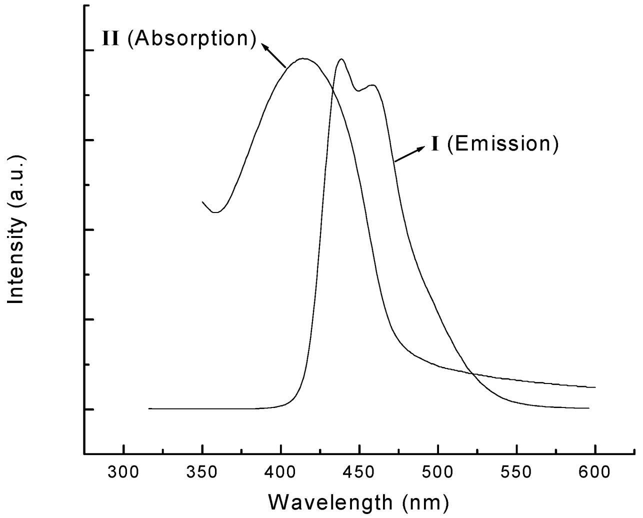

Figure 7. Spectral overlap between emission of polymer **I** and absorption of polymer **II**.

Effect of Film Thickness on Photoluminescence. Solid-state PL spectra were acquired from polymer films on glass plates. Comparison between Figure 4 and Figure 2b showed that the emission spectra of polymer **II** films were red-shifted by 64−101 nm from that of the polymer **II** solution, indicating clearly that a stronger intermolecular interaction occurred in the solid state. In addition, the vibronic fine structures observed in solution PL spectra disappeared in the film spectra. To probe the impact of film thickness on luminescent properties, a polymer **II** chloroform solution was spin-coated onto glass substrates at different speeds. As shown in Figure 4, PL spectra of the films showed a small red shift (∼ 5 nm) as the film thickness was increased from 55 to 180 nm. To obtain a very thick film, the polymer **II** solution was directly cast on a glass substrate and the chloroform solvent was allowed to evaporate slowly at room temperature in a nitrogen atmosphere. The PL spectrum of the resulting 17 μm

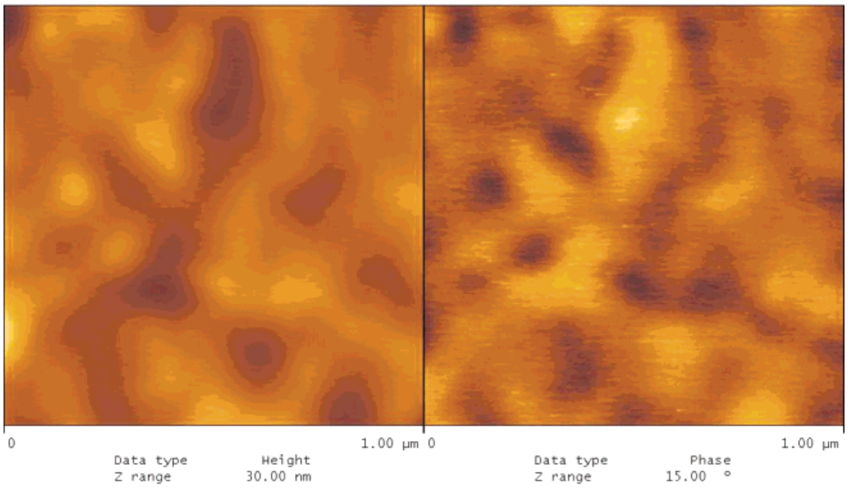

Figure 8. AFM images of the 75 nm spin-coated film for polymer blend.

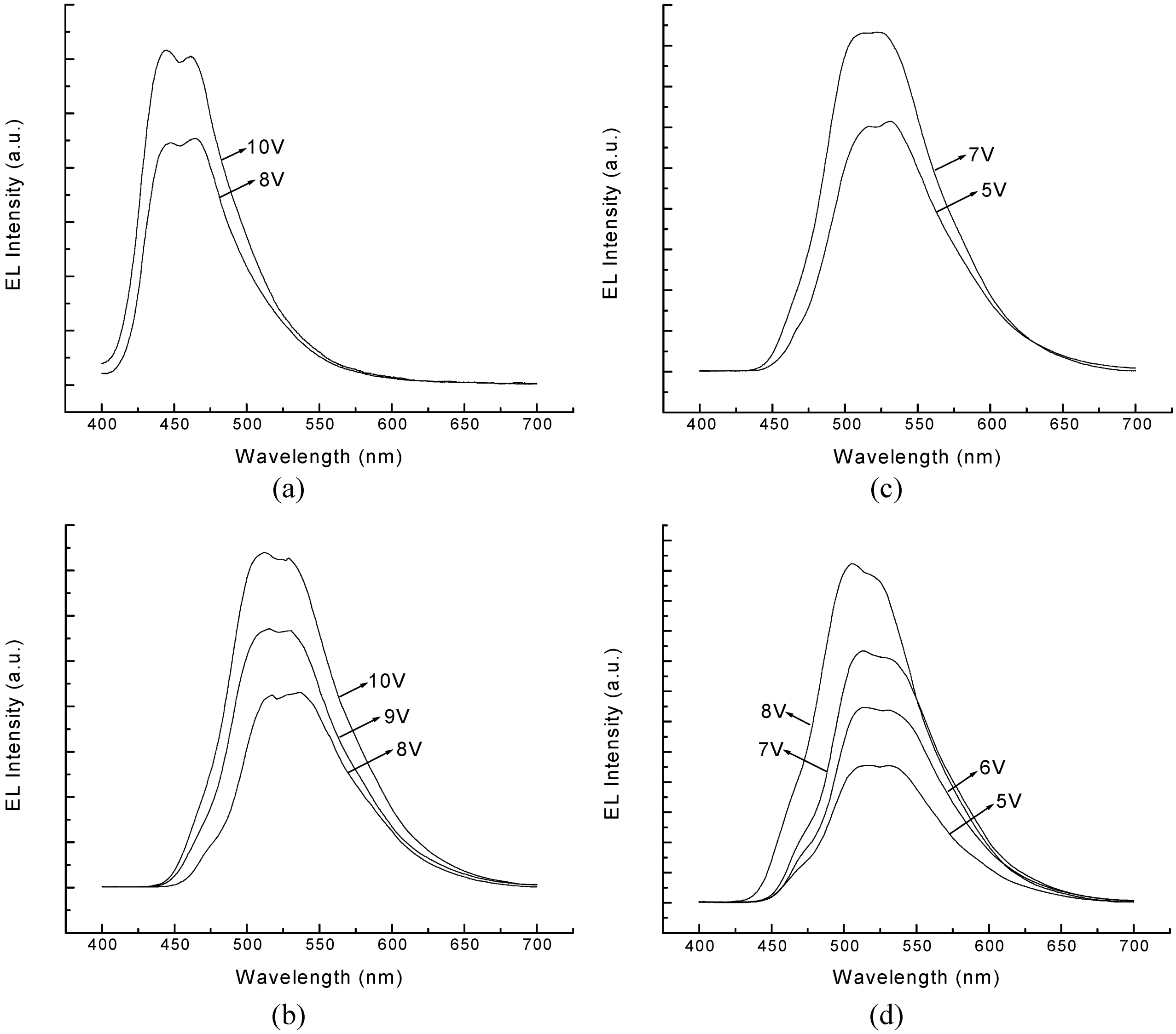

Figure 9. Electroluminescence spectra for LEDs at different voltages: (a) ITO/PEDOT/**I**/Ca; (b) ITO/**II**/Ca; (c) ITO/PEDOT/**II**/Ca; (d) ITO/PEDOT/blend/Ca.

thick film shows a 37 nm red shift compared to that of a 55 nm spin-coated film (see Table 4). The large red shift is explained by considering molecular packing. In the process of making thick films, the solvent evaporates slowly, and the chains are able to achieve an equilibrium morphology, adopting energetically more favorable conformations. Thus, under photoexcitation excitons can freely migrate and be transformed into lower energy states and finally yield a red-shifted emission. Consideration of molecular packing also explains the slight bathochromic shift observed for the thicker spin-cast films. For a given polymer solution, a thicker spin-coated film requires a slower spinning speed, which results in a lower centrifugal force and permits the achievement of molecular packing closer to equilibrium.

Photoluminescence and Electroluminescence of Polymer Blend Film: Förster Energy Transfer Phenomena. Compared to the PL spectra of the polymer blend solution (**I**:**II** = 1:1, weight ratio) which emit violet-blue light, the polymer blend film displays a green emission at 507 nm, resembling the PL spectrum of polymer **II** film in shape as shown in Figure 5. This observation indicates that a complete Förster energy transfer from polymer **I** to polymer **II** occurred in the film. Under different wavelength photoexcitation, the blend emits the same green light (see Table 5), demonstrating that the energy transfer is independent of excitation wavelength. The PL spectra of the blend shows a small blue shift (7 nm) compared to polymer **II,** suggesting that the excitons born on polymer **I** chains will migrate to polymer **II** chains and possess a higher energy than those born on polymer **II** chains, thus yielding a higher energy emission.

The EL spectra of polymer **I**, polymer **II**, and the blend (**I**:**II** = 1:1, weight ratio) are shown in Figure 6. The EL peak wavelengths are listed in Table 6. The EL spectra of double-layer LEDs exhibited small red shifts, which results from interfacial effects. For both single-layer and double-layer devices, the polymer blend displays green emission and the EL spectra of the blend are quite similar to that of polymer **II**, indicating again a complete Förster energy transfer between the two polymers.

Two conditions are necessary for realizing efficient Förster energy transfer between two polymers: sufficient spectral overlap between the emission of the higher band-gap polymer and the absorption of the lower band-gap polymer, and uniform mixing on a few nanometer scale of the two polymers.[43] In this study, the emission spectrum of polymer **I** and the absorption spectrum of polymer **II** do overlap significantly in the range of 400−500 nm (Figure 7). The *m*-phenylenevinylene units in both molecular structures (Figure 1) and the hexyloxy side chains facilitate the near miscibility of the two polymers. The AFM image (Figure 8) for the polymer blend film shows no obvious phase separation. These observations are consistent with the complete Förster energy transfer phenomenon in the PL and EL seen in the polymer blend film.

Effect of Applied Voltage on Electroluminescence Spectra. The EL spectra as a function of applied voltage for ITO/PEDOT/**I**/Ca, ITO/**II**/Ca, ITO/PEDOT/**II**/Ca, and ITO/PEDOT/blend/Ca devices are shown in Figure 9 with the EL peak wavelengths listed in Table 7. In Figure 9a, 448 and 444 nm peaks can be attributed to the vibronic 0−0 transition; 464 and 461 nm peaks to the 0−1 transition. In Figure 9b, the 518, 516, and 512 nm peaks are associated with the 0−1 transition, and the 537, 530, and 529 nm peaks with the 0−2 transition. Similarly in Figure 9c, the 517 and 514 nm peaks derive from the 0−1 transition, 531 and 522 nm from the 0−2 transition. With an increase of applied voltage, all the EL spectra show a blue shift, and the emission intensity of the higher energy transition increases at the expense of the lower energy transition. This phenomenon is related to Joule heating in the LED, which results in a thermochromic effect.[44] Additionally, band-gap distributions in the polymer can contribute to the effect;[45] at higher applied voltage, emission from the higher band-gap segments contributes more to the total emission. For the ITO/PEDOT/blend/Ca device, all the EL spectra resemble that of the ITO/**II**/Ca and ITO/PEDOT/**II**/Ca devices in shape (Figure 9d). The 506−517 nm peaks derive from the 0−1 transition and the 521−531 nm peaks from the 0−2 transition. The ITO/PEDOT/blend/Ca LED only emits green light under different voltages, showing that Förster energy transfer process in LEDs is independent of applied voltage.

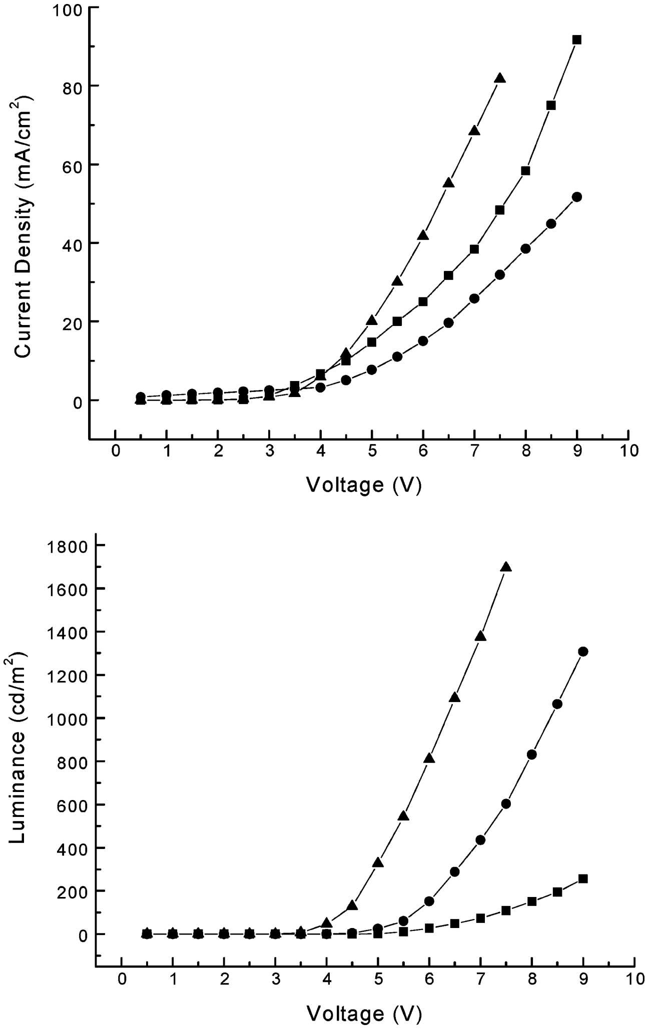

Figure 10. Current density and luminance vs applied voltage for ITO/PEDOT/**I**/Ca (■), ITO/PEDOT/blend/Ca (●), and ITO/PEDOT/**II**/Ca (▲) devices.

Current−Voltage-Luminance Characteristics. The turn-on voltage at which the LED reaches the “flat-band” condition depends only upon the band gap of the polymer and the work function of the electrodes.[46] For given electrodes, we can compare the band gap difference for different emissive polymer layers in the LEDs from these values. The turn-on voltages of ITO/PEDOT/**I**/Ca, ITO/PEDOT/**II**/Ca, and ITO/PEDOT/blend/Ca devices are 4.5, 3.5, and 4.5 V respectively (Figure 10). The polymer blend shows the same turn-on voltage as polymer **I**, suggesting that the high band gap polymer in the blend will determine the effective band gap and affect the turn-on voltage of the device. The external quantum efficiencies of the LEDs are 0.083%, 0.91% and 1.33% respectively. Thus, the polymer blend provides more efficient electroluminescence indicating that polymer **I** also acts as a medium to reduce exciton quenching. The chromophore blend aids the separation of PL output from absorption, thereby alleviating self-absorption and improving the EL efficiency.

Conclusion

With increase of excitation wavelength, chromophore concentration of the polymer solution and the thickness of conjugated polymer film, the PL spectra show a red shift. Förster energy transfer between higher band-gap polymer **I** and lower band-gap polymer **II** is complete and is independent of the excitation wavelength and the applied voltage. With increase of applied voltage, EL spectra show a blue shift, and the emission intensity for higher energy transition increases at the expense of lower energy transition. The polymer blend LEDs show improved efficiency as polymer **I** reduces exciton quenching.

Acknowledgment. This work was supported by the Air Force Office of Scientific Research (Grant No. F49620-99-1-002). We acknowledge the help of MRSEC at the University of Massachusetts Amherst in providing access to the AFM facility.

References and Notes

(1) Heeger, A. J. *Angew. Chem., Int. Ed.* **2001**, *40*, 2591.
(2) Burroughes, J. H.; Bradley, D. D. C.; Brown, A. R.; Marks, R. N.; Mackay, K.; Friend, R. H.; Burns, P. L.; Holmes, A. B. *Nature (London)* **1990**, *347*, 539.
(3) Sarker, A. R.; Ding, L.; Lahti, P. M.; Karasz, F. E. *Macromolecules* **2002**, *35*, 223.
(4) Zheng, M.; Ding, L.; Karasz, F. E. *Macromol. Chem. Phys.* **2002**, *203*, 1337.
(5) Chu, Q.; Pang, Y.; Ding, L.; Karasz, F. E. *Macromolecules* **2002**, *35*, 7569.
(6) (a) Zhang, X.; Kale, D. M.; Jenekhe, S. A. *Macromolecules* **2002**, *35*, 382. (b) Zheng, M.; Ding, L.; Gürel, E. E.; Lahti, P. M.; Karasz, F. E. *Macromolecules* **2001**, *34*, 4124.
(7) Friend, R. H.; Gymer, R. W.; Holmes, A. B.; Burroughes, J. H.; Marks, R. N.; Taliani, C.; Bradley, D. D. C.; Dos Santos, D. A.; Brédas, J. L.; Lögdlund, M.; Salaneck, W. R. *Nature (London)* **1999**, *397*, 121.
(8) Kraft, A.; Grimsdale, A. C.; Holmes, A. B. *Angew. Chem., Int. Ed.* **1998**, *37*, 402.
(9) Pei, Q.; Yu, G.; Zhang, C.; Yang, Y.; Heeger, A. J. *Science* **1995**, *269*, 1086.
(10) Ding, L.; Jonforsen, M.; Roman, L. S.; Andersson, M. R.; Inganäs, O. *Synth. Met.* **2000**, *110*, 133.
(11) Yang, Y.; Heeger, A. J. *Nature (London)* **1994**, *372*, 344.
(12) Hide, F.; Díaz-García, M. A.; Schwartz, B. J.; Andersson, M. R.; Pei, Q.; Heeger, A. J. *Science* **1996**, *273*, 1833.
(13) Burn, P. L.; Holmes, A. B.; Kraft, A.; Bradley, D. D. C.; Brown, A. R.; Friend, R. H.; Gymer, R. W. *Nature (London)* **1992**, *356*, 47.
(14) Yang, Z.; Sokolik, I.; Karasz, F. E. *Macromolecules* **1993**, *26*, 1188.
(15) Andersson, M. R.; Berggren, M.; Gustafsson, G.; Hjertberg, T.; Inganäs, O.; Wennerström, O. *Synth. Met.* **1995**, *71*, 2183.
(16) Hu, B.; Yang, Z.; Karasz, F. E. *J. Appl. Phys.* **1994**, *76*, 2419.
(17) Zhang, C.; von Seggern, H.; Pakbaz, K.; Kraabel, B.; Schmidt, H.-W.; Heeger, A. J. *Synth. Met.* **1994**, *62*, 35.
(18) Hu, B.; Zhang, N.; Karasz, F. E. *J. Appl. Phys.* **1998**, *83*, 6002.
(19) McGehee, M. D.; Bergstedt, T.; Zhang, C.; Saab, A. P.; O'Regan, M. B.; Bazan, G. C.; Srdanov, V. I.; Heeger, A. J. *Adv. Mater.* **1999**, *11*, 1349.
(20) Romero, D. B.; Schaer, M.; Zuppiroli, L.; Cesar, B.; Francois, B. *Appl. Phys. Lett.* **1995**, *67*, 1659.
(21) Hu, B.; Karasz, F. E. *Chem. Phys.* **1998**, *227*, 263.
(22) Yu, G.; Nishino, H.; Heeger, A. J.; Chen, T.-A.; Rieke, R. D. *Synth. Met.* **1995**, *72*, 249.
(23) Nishino, H.; Yu, G.; Heeger, A. J.; Chen, T.-A.; Rieke, R. D. *Synth. Met.* **1995**, *68*, 243.
(24) Cleave, V.; Yahioglu, G.; Le Barny, P.; Friend, R. H.; Tessler, N. *Adv. Mater.* **1999**, *11* (4), 285.
(25) Förster, T. *Discuss. Faraday Soc.* **1959**, *27*, 7.
(26) Agranovich, V. M.; Galanin, M. D. *Electronic Excitation Energy Transfer in Condens. Matter*; North-Holland: Amsterdam, 1982.
(27) Deshpande, R. S.; Bulović, V.; Forrest, S. R. *Appl. Phys. Lett.* **1999**, *75*, 888.
(28) Tasch, S.; List, E. J. W.; Ekström, O.; Graupner, W.; Leising, G.; Schlichting, P.; Rohr, U.; Geerts, Y.; Scherf, U.; Müllen, K. *Appl. Phys. Lett.* **1997**, *71*, 2883.
(29) Lee, T.; Park, O.; Cho, H.; Hong, J.; Kim, C.; Kim, Y. *Synth. Met.* **2001**, *122*, 437.
(30) Hu, B.; Karasz, F. E. *J. Appl. Phys.* **2003**, *93*, 1995.
(31) Gupta, R.; Stevenson, M.; Heeger, A. J. *J. Appl. Phys.* **2002**, *92*, 4874.
(32) Jiang, X.; Jen, A. K. Y.; Carlson, B.; Dalton, L. R. *Appl. Phys. Lett.* **2002**, *81*, 3125.
(33) Chen, F.; Yang, Y.; Thompson, M. E.; Kido, J. *Appl. Phys. Lett.* **2002**, *80*, 2308.
(34) Stork, M.; Gaylord, B. S.; Heeger, A. J.; Bazan, G. C. *Adv. Mater.* **2002**, *14*, 361.
(35) Nguyen, T.; Wu, J.; Tolbert, S. H.; Schwartz, B. J. *Adv. Mater.* **2001**, *13*, 609.
(36) Montali, A.; Palmans, A. R. A.; Bras, J.; Pepin-Donat, B.; Guillerez, S.; Smith, P.; Weder, C. *Synth. Met.* **2000**, *115*, 41.
(37) Liao, L.; Pang, Y.; Ding, L.; Karasz, F. E. *Macromolecules* **2001**, *34*, 7300.
(38) Liao, L.; Pang, Y.; Ding, L.; Karasz, F. E. *Macromolecules* **2002**, *35*, 6055.
(39) Jenekhe, S. A.; Osaheni, J. A. *Science* **1994**, *265*, 765.
(40) (a) Halkyard, C. E.; Rampey, M. E.; Kloppenburg, L.; Studer-Martinez, S. L.; Bunz, U. H. F. *Macromolecules* **1998**, *31*, 8655. (b) Morisaki, Y.; Chujo, Y. *Macromolecules* **2002**, *35*, 587.
(41) Chandross, E. A.; Dempster, C. J. *J. Am. Chem. Soc.* **1970**, *92*, 3586.
(42) Li, H.; Powell, D. R.; Hayashi, R. K.; West, R. *Macromolecules* **1998**, *31*, 52.
(43) Dogariu, A.; Gupta, R.; Heeger, A. J.; Wang, H. *Synth. Met.* **1999**, *100*, 95.
(44) Braun, D.; Moses, D.; Zhang, C.; Heeger, A. J. *Appl. Phys. Lett.* **1992**, *61*, 3092.
(45) Bolognesi, A.; Bajo, G.; Paloheimo, J.; Östergård, T.; Stubb, H. *Adv. Mater.* **1997**, *9* (2), 121.
(46) Parker, I. D. *J. Appl. Phys.* **1994**, *75*, 1656.

MA030237Q